Identification of Novel Interaction between Annexin A2 and Keratin 17

EVIDENCE FOR RECIPROCAL REGULATION[*][S]

Byung-Min Chung[‡], **Christopher I. Murray**[§], **Jennifer E. Van Eyk**[§¶], **and Pierre A. Coulombe**[‡§||1]

From the [‡]*Department of Biochemistry and Molecular Biology, Bloomberg School of Public Health, the* [§]*Department of Biological Chemistry, School of Medicine, the* [¶]*Department of Medicine, Division of Cardiology, Johns Hopkins Bayview Proteomic Center, and the* [||]*Department of Dermatology, School of Medicine, Johns Hopkins University, Baltimore, Maryland 21205*

Background: Expression of EGFR, K17, and AnxA2 are correlated in cancer settings.
Results: AnxA2 and K17 physically interact and undergo reciprocal regulation controlled in part by EGFR signaling.
Conclusion: K17 serves as a regulator of the signaling pathway involving AnxA2, whereas AnxA2 regulates K17 stability.
Significance: This study demonstrates a novel interaction and reciprocal regulation between AnxA2 and K17.

Keratins are cytoplasmic intermediate filament proteins providing crucial structural support in epithelial cells. Keratin expression has diagnostic and even prognostic value in disease settings, and recent studies have uncovered modulatory roles for select keratin proteins in signaling pathways regulating cell growth and cell death. Elevated keratin expression in select cancers is correlated with higher expression of EGF receptor (EGFR), whose overexpression and/or mutation give rise to cancer. To explore the role of keratins in oncogenic signaling pathways, we examined the regulation of epithelial growth-associated keratin 17 (K17) in response to EGFR activation. K17 is specifically up-regulated in detergent-soluble fraction upon EGFR activation, and immunofluorescence analysis revealed alterations in K17-containing filaments. Interestingly, we identified AnxA2 as a novel interacting partner of K17, and this interaction is antagonized by EGFR activation. K17 and AnxA2 proteins show reciprocal regulation. Modulating expression of AnxA2 altered K17 stability, and AnxA2 overexpression delays EGFR-mediated change in K17 detergent solubility. Down-regulation of K17 expression, in turn, results in decreased AnxA2 phosphorylation at Tyr-23. These findings uncover a novel interaction involving K17 and AnxA2 and identify AnxA2 as a potential regulator of keratin filaments.

The keratin family of intermediate filament proteins provides crucial structural support for epithelial cells upon mechanical and non-mechanical stresses. The 54 keratin genes, with 28 type I and 26 type II sequences, are tightly regulated in a pairwise, tissue- and differentiation-specific, and evolutionarily conserved manner (1). Type I and II keratins initially heterodimerize as they undergo polymerization into 10- to 12-nm-wide filaments, leading to a requirement for pairwise regulation at the transcriptional and posttranscriptional levels (2). Keratin filaments can be dynamically remodeled and undergo reorganization upon various mechanical and non-mechanical stimuli. Mutation-based defects in keratin filament structure, organization, and/or regulation result in epithelial fragility and cause skin blistering conditions such as epidermolysis bullosa simplex (EBS)[2] (3, 4).

Many studies have revealed roles for keratins beyond their mechanical support function. In particular, the wound-induced K17 regulates protein synthesis and cell growth signaling through binding to the adapter protein 14-3-3σ and translation elongation factor subunit eEF1Bγ (5, 6). Moreover, higher K17 expression has been correlated with tumor progression and poorer prognosis (7). Recently, K17 has been found to impact the onset of skin tumorigenesis by modulating the immune response (8). Interestingly, K17 expression has also been correlated with epidermal growth factor receptor (EGFR) expression *in vivo* (7). Indeed, previous studies showed that EGFR activation results in the stimulation of K17 promoter activity, along with that of K6 and K16, two additional wound-induced keratins (9–11). Keratin may also affect EGFR activity because a transgenic mouse model with constitutive expression of K16 showed a higher EGFR phosphorylation level in neonatal skin compared with nontransgenic littermates (12). Proteomic studies also showed that activated EGFR and K17 may exist as a complex (13, 14). Despite these efforts, however, the impact that EGFR may have on the roles and regulation of K17, and *vice versa*, remain poorly defined. This issue is clinically significant, as EGFR and K17 expression often occurs in the subset of breast cancer patients who lack therapeutic targets (7). Understanding the functional relationship between these two proteins might help devise novel targeted therapies for cancer patients. Here we report our efforts to examine this relationship. We identify annexin A2 (AnxA2) as a novel keratin-interacting protein, and

---

[S] This article contains supplemental Figs. S1–S7 and Table S1.

[1] To whom correspondence should be addressed: Department of Biochemistry and Molecular Biology, Johns Hopkins Bloomberg School of Public Health, 615 N. Wolfe St., Room W8041, Baltimore, MD 21205. Tel.: 410-955-3671; Fax: 410-955-2926; E-mail: coulombe@jhsph.edu.

[2] The abbreviations used are: EBS, epidermolysis bullosa simplex; K17, keratin 17; EGFR, EGF receptor; AnxA2, annexin A2; IS, Triton-insoluble; TS, Triton-soluble.

establish that AnxA2 and K17 mutually regulate one another in the setting of EGFR-induced biological responses.

EXPERIMENTAL PROCEDURES

Plasmids—Plasmids pET-K6 and pET-K17[3] were used to express human keratins as recombinant proteins in *Escherichia coli*. The mammalian expression constructs pEGFP-C3 K5 (16) and pEGFP-C3 K17 (17) have been described. AnxA2 cDNA was cloned out of pOTB7 AnxA2 (ATCC) using PCR with the primers 5′-A<u>GTCGAC</u>GATGTCTACTG TTCACG-3′ (forward) (with a SalI restriction site underlined) and 5′-GT<u>GGATCC</u>TCAGTCA-TCTC CACC-3′ (reverse) (with a BamHI restriction site underlined) and cloned into mCherry-C1 (Clontech, Mountain View, CA). To silence K17 expression, shRNAs targeting K17 cDNA at positions 387 (designated K17C) or 411 (K17D) were devised. Oligonucleotides 5′-GATCCCC <u>GGAGGAGCTGGCCTACCT-GAATTCAAGAGA</u>TTCAGGTAGGCCAGCTCCTCCTTT-TTA-3′ (forward) and its complement 5′-AGCTTAAAAA<u>GGA-GGAGCTGGCCTACCTGAATCTCTTGAATTCAGGTAGG-CCAGCTCCTCC</u>GGG-3′ (reverse) were used as inserts for K17C, whereas 5′-GATCCCC<u>GAACCACGAGGAGGAGATG-AA</u>TTCAAGAGA<u>TTCATCTCCTCCTCGTGGTTC</u>TTT-TTA-3′ and 5′-AGCTTAAAAA<u>GAACCACGAGGAGGA-GATGAA</u>TCTCTTGAA<u>TTCATCTCCTCCTCGTGGTT-C</u>GGG-3′ were used for K17D (K17 targeting sequences underlined). To silence AnxA2 expression, oligonucleotides 5′-GATCCCC<u>GGTCTGAATTCAAGAGAAAGTTTCAAGA-GA</u>ACTTTCTCTTGAATTCAGACCTTTTTA-3′ (forward) and its complement 5′-AGCTTAAAAA<u>GGTCTGAATTCA-AGAGAAAGT</u>TCTCTTGAA<u>ACTTTCTCTTGAATTCAG-ACC</u>GGG-3′ (reverse) were used (AnxA2 targeting sequences described previously in Ref. 18 are underlined). Inserts were cloned in pSuper.retro.puro vector (OligoEngine, Seattle, WA). The non-sense shRNA control pSuper.retro.puro NS has been described previously (19).

Cell Culture and EGF Stimulation—A431, BT-20, and BHK-21 (ATCC) cells were grown in Dulbecco's modified essential medium (Invitrogen) containing 10% FBS (Atlanta Biologicals, Lawrenceville, GA), 100 units/ml penicillin, and 100 μg/ml streptomycin (Invitrogen) at 37 °C in 5% CO$_2$. Primary cultures of skin keratinocytes from 2-day-old mouse pups that are either heterozygous ($K17^{+/-}$) or homozygous ($K17^{-/-}$) for a *K17* null allele were isolated and cultured as described previously (20). For EGF stimulation, cells previously incubated for 18 h in 0.1% FBS-containing medium were either left untreated or treated with 100 ng/ml EGF for the indicated time periods.

Antibodies and Other Reagents—The following antibodies were obtained from commercial sources: rabbit polyclonal anti-EGFR (1005), mouse mAb anti-annexin II (C-10), anti-phospho-annexin II (Y24), and anti-GAPDH (1D4) were from Santa Cruz Biotechnology (Santa Cruz, CA). mAb anti-phosphotyrosine (4G10) was from Millipore (Billerica, MA). Anti-phospho-K17 (S44) was from Cell Signaling Technology (Danvers, MA). mAb anti-β actin (Clone AC-15) was from Sigma-Aldrich (St Louis, MO). mAb anti-K5 (AF138) was from Covance

(Princeton, NJ). pAb anti-K17 and anti-K6 were described previously (21). Purified human EGF was from Sigma-Aldrich. EGFR inhibitor Erlotinib was from LC Laboratories (Woburn, MA). All other chemicals were from Sigma-Aldrich unless noted otherwise.

Retroviral Infections—Retroviral supernatants were generated by calcium phosphate-mediated cotransfection of the shRNA plasmids and the packaging plasmids into the packaging cell line Phenix as described (19). The supernatants, collected 24 h after transfection, were used to infect subconfluent cells in three sequential 4-h incubations in the presence of 4 μg/ml polybrene (Sigma-Aldrich). Transductants were selected in puromycin (0.5 μg/ml), beginning 48 h after infection.

Preparation of Cell Lysates, Protein Gel Electrophoresis, and Immunoblotting—Cells were washed with phosphate-buffered saline and prepared in cold Triton lysis buffer (1% Triton X-100; 40 mM HEPES (pH 7.5); 120 mM sodium chloride; 1 mM ethylene diamine-tetraacetic acid; 1 mM phenyl methylsulfonyl fluoride; 10 mM sodium pyrophosphate; 1 μg/ml each of cymostatin, leupeptin, and pepstatin; 10 μg/ml each of aprotinin and benzamidine; 2 μg/ml antipain; 1 mM sodium orthovanadate; 50 mM sodium fluoride). To isolate detergent-insoluble proteins, the insoluble material following Triton lysis buffer incubation was pelleted, washed with PBS, and dissolved in urea lysis buffer (6.5 M urea; 50 mM Tris (pH 7.5); 1 mM ethylene glycol tetraacetic acid; 2 mM dithiothreitol; 1 mM phenylmethylsulfonyl fluoride; 1 μg/ml each of cymostatin, leupeptin, and pepstatin; 10 μg/ml each of aprotinin and benzamidine; 2 μg/ml antipain; 50 mM sodium fluoride). For analyses of total protein pool as reported in Fig. 2, cells were lysed directly in the urea lysis buffer.

For immunoblotting, cell lysates were prepared in Laemmli SDS-PAGE sample buffer, and protein concentration was determined using the Bio-Rad protein assay (Bio-Rad) with bovine serum albumin as standard. Aliquots of protein lysate were resolved by SDS-PAGE, transferred to nitrocellulose membranes (0.45 μm) (Bio-Rad), and immunoblotted with the indicated antibodies followed by HRP-conjugated goat anti-mouse or goat anti-rabbit IgG (Sigma) and Pierce ECL Western blotting substrate (Thermo Scientific, Hudson, NH). Signals were detected using Konica Minolta SRX-101A film developer (Figs. 1 and 4A) or the FluorChem Q imaging system (Cell Biosciences, Santa Clara, CA) (Figs. 2, 3, 4B, and 5–7). For Western blot signal quantitation, ImageJ or Alphaview (Cell Biosciences) software was used.

Immunoprecipitation—Cell lysates were prepared as described above, except that the lysis buffer also contained 2% Empigen. Aliquots of cell lysate were incubated with anti-K17 antibody or preimmune serum control, and immune complexes were captured using the TrueBlot anti-rabbit Ig immunoprecipitation beads (eBioscience, San Diego, CA). Subsequent SDS-PAGE and immunoblotting were performed as above, except that the rabbit TrueBlot anti-rabbit IgG HRP (eBioscience) was used for K17 blots.

High-speed Cosedimentation Assay—Recombinant keratin expression, purification and *in vitro* filament assembly were described previously (22). Assembled keratin filaments were

---

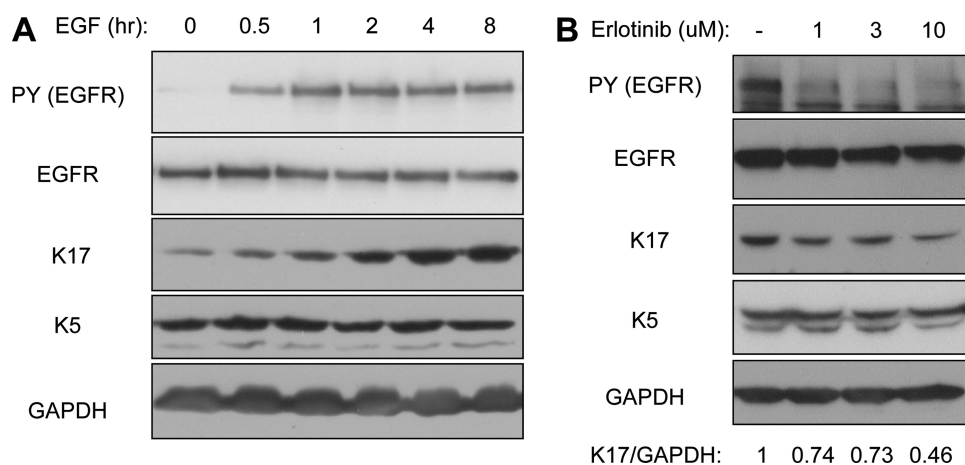[3] J. E. Rotty and P. A. Coulombe, submitted for publication.

FIGURE 1. **EGFR increases K17 protein levels.** A431 cells were growth factor-deprived prior to 100 ng/ml EGF treatment for the indicated time periods (*A*) or incubated with various concentrations of EGFR inhibitor Erlotinib for 2 h (*B*). Whole cell lysates were prepared in Triton lysis buffer, and immunoblotting was performed with antibodies against the indicated proteins. Anti-phosphotyrosine (*PY*) 4G10 antibody was used to show EGFR activity. K17 and GAPDH signal intensities were quantified using ImageJ software.

then incubated with or without purified bovine AnxA2 (Genway, San Diego, CA) or Src catalytic domain (a kind gift from Dr. John Kuriyan, University of California, Berkeley, CA) for 30 min at room temperature before subjecting the samples to high-speed centrifugation as described (23). Supernatants were separated from pellets, and both fractions were resolved and analyzed using SDS-PAGE and Western blotting.

Immunofluorescence Staining and Confocal Microscopy—For immunostaining, cells grown on glass coverslips (VWR, Batavia, IL) were washed in PBS and fixed in ice-cold methanol for 20 min at −20 °C. Samples were then blocked in 5% normal goat serum in PBS for 18 h at 4 °C before staining with primary antibodies diluted in blocking buffer for 1 h followed by Alexa Fluor 488- or Alexa Fluor 647-conjugated goat anti-mouse or goat anti-rabbit secondary antibodies (Invitrogen) for 1 h. Coverslips were mounted on microscope slides with mounting media containing 1,4-diaza-bicyclo[2.2.2]octane. Confocal fluorescence images were obtained with a LSM510 fluorescence confocal microscope (Carl Zeiss, Thornwood, NY) under a ×63 oil immersion lens.

RESULTS

K17 Is Up-regulated following EGFR Activation—We first monitored K17 protein levels upon EGFR activation. The human epidermoid carcinomas cell line A431 was used for this purpose because of its high EGFR expression and constitutive expression of K17. When growth factor-deprived A431 cells were stimulated with EGF to activate EGFR, levels of K17 antigens increased within 30 min (Fig. 1*A*). Interestingly, EGF-induced increase of K17 protein was highly specific, as its type II dimerizing partner in this setting, K5, remained at the same level. The requirement for EGFR activity in this K17 up-regulation was established by treating A431 cells with the inhibitor Erlotinib, resulting in decreased levels of K17 (Fig. 1*B*). Similar to EGFR activation, EGFR inhibition had no effect on K5 cellular levels.

EGFR-dependent Change in K17 Solubility and Filament Reorganization—We next examined the status of K17-containing keratin filaments upon EGFR activation. Growth factor-

deprived A431 cells were stimulated with EGF and processed for K17 indirect immunofluorescence (Fig. 2*A* and supplemental Fig. S1). Untreated control showed distinct K17-containing filaments largely organized in bundles concentrated in the perinuclear region. In contrast, EGF-stimulated cells showed a more dispersed and "fuzzy" staining pattern for K17, suggesting that a fraction of the K17 protein pool had redistributed to a soluble (non-filamentous) form.

To further characterize the EGF-induced changes in K17 filament network, we examined keratin solubility to the detergent Triton X-100 as a reflection of a soluble *versus* filament-bound status. Following EGF stimulation, cell lysates were obtained with Triton-based lysis buffer as done in studies reported in Fig. 1, and a high-speed centrifugation was performed. Triton-soluble supernatants were recovered, and Triton-insoluble pellets were washed and dissolved in urea-based lysis buffer. A duplicate set of cells was processed directly in urea-based lysis buffer to yield a total protein reference. This analysis showed that EGF stimulation specifically increased the Triton-soluble pool of K17 but did not impact the Triton-insoluble pool (Fig. 2*B*). No effect was seen on K5 partitioning (Fig. 2*B*). Quantitation of several immunoblot analyses reflecting independent assays ($n = 7$) confirmed this result (Fig. 2*C*). Together, these findings show that the increase in K17 protein levels brought about by EGFR activation mainly takes place in the soluble pool compartment (which is small relative to the total keratin protein pool; see the legend for Fig. 2*B* and Ref. 20), and correlates with a remodeling of K17-containing filaments.

AnxA2 Interacts with K17 Filaments—To identify factor(s) contributing to EGFR-mediated change in K17 filaments, we screened for K17-binding partners through immunoprecipitation coupled with mass spectroscopy (supplemental Fig. S2 and Table S1). This effort yielded AnxA2 as a novel K17-binding partner. AnxA2 is a phospholipid-binding protein that has been implicated previously in the regulation of actin cytoskeleton dynamics (24) and keratin filament stability (25). Furthermore, a heteromeric complex comprising AnxA2 and p11 (also known as S100A10) has been shown to bind glial fibrillary
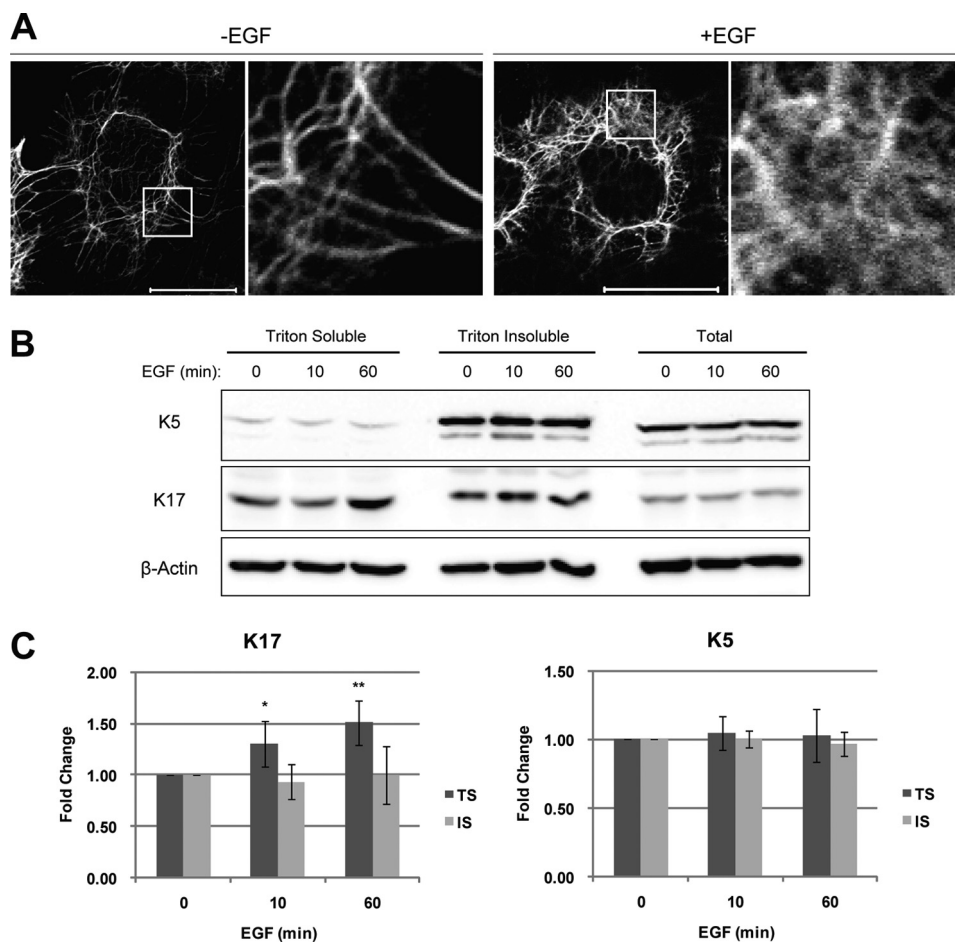
FIGURE 2. **EGFR activation alters K17 solubility.** *A*, growth factor-deprived A431 cells were treated with (+EGF) or without (-EGF) 100 ng/ml EGF for 1 h and then immunostained with an anti-K17 antibody. *Scale bar* = 20 μm. Boxed-in areas are enlarged on the right. *B*, growth factor-deprived A431 cells were treated with 100 ng/ml EGF for the indicated time periods. Whole cell lysates were processed for Triton solubility. Immunoblotting was performed with antibodies against the indicated proteins. *C*, K17 and K5 signal intensities from *B* were quantified using the AlphaView SA software. *TS* indicates Triton soluble, whereas *IS* indicates Triton insoluble pool. *, $p < 0.006$; **, $p < 0.0003$ compared with 0 min TS.

acidic protein, a type III intermediate filament protein, and stimulate its assembly (26). Therefore, we next sought to confirm the AnxA2-K17 interaction. When overexpressed in the human embryonic kidney cell line 293T, AnxA2 coimmunoprecipitated with K17 but not preimmune serum control, indicating that AnxA2 is a K17-binding protein in this setting (Fig. 3*A*). Endogenous AnxA2 also coimmunoprecipitated with endogenous K17 in A431 cells (Fig. 4*B*). Next, we compared the intracellular distribution of AnxA2 and K17 by expressing fluorescent protein-tagged AnxA2 (mCherry) and K17 (GFP) in A431 cells (Fig. 3*B*). AnxA2 localized mostly in the cytoplasm as well as at the plasma membrane, whereas GFP-tagged K17 was part of a cytoskeletal network and enriched in the perinuclear area, as described above. Instances of colocalization between AnxA2 and K17 were observed in punctate, discrete spots along the K17 filament network (Fig. 3*B*, *inset*), indicating close physical localization of the two proteins. Controls using mCherry-AnxA2 and GFP or mCherry and GFP-K17 showed fewer colocalizations, as expected (supplemental Fig. S3).

Although coimmunoprecipitation and fluorescence imaging analyses showed that AnxA2 and K17 may be part of a complex, it did not address whether the interaction between them is direct or indirect. A high speed cosedimentation assay with

purified proteins was performed *in vitro* to test for a direct interaction between K17-containing filaments and AnxA2 (Fig. 3*C*). By itself, AnxA2 partitioned mostly to the supernatant fraction after high-speed centrifugation. Upon incubation with reconstituted K6/K17 filaments, however, AnxA2 copelleted with keratins, indicating that AnxA2 can interact directly with keratin filaments. In contrast, the catalytic domain of Src (Src-CD) showed a minimal degree of interaction with K6/K17 filaments, as shown previously[3]. We also found that AnxA2 coimmunoprecipitated with K5 (supplemental Fig. S4), suggesting that the interaction of AnxA2 with K17 may involve a type II keratin partner. Together, these findings establish that AnxA2 interacts with K17 and/or K17-containing filaments *in vitro* and *in vivo*.

EGFR-mediated Dissociation of AnxA2 from K17—Because the detergent-soluble pool of K17 is sensitive to EGFR activity (Fig. 2) and in light of the binding of AnxA2 to K17 filaments (Fig. 3), we next tested whether EGFR activity could affect the AnxA2/K17 interaction. We find that the amount of AnxA2 present in the keratin-rich Triton-insoluble pool (IS) decreased following EGF stimulation (Fig. 4*A*). Moreover, relative to unstimulated A431 cells, from which one can readily coimmunoprecipitate an endogenous AnxA2/K17
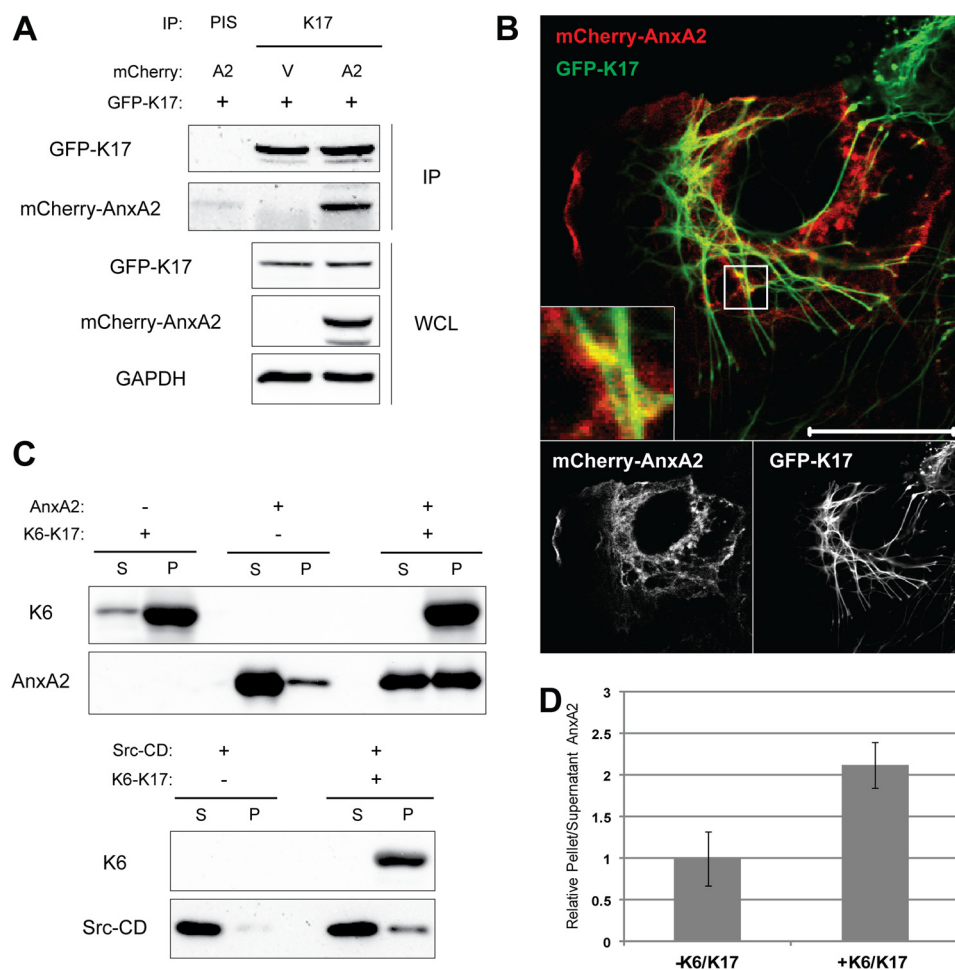
FIGURE 3. **AnxA2 is a K17-binding protein.** *A*, mCherry-tagged AnxA2 (*A2*) or vector control (*V*) and GFP-K17 were expressed in 293T cells. Immunoprecipitation was performed with anti-K17 antibody (*K17*) or preimmune serum (*PIS*) as a control, and immunoblotting was performed with antibodies against the indicated proteins. *B*, mCherry-AnxA2 and GFP-K17 were expressed in A431 cells, and fluorescent images were taken with confocal microscopy. *Scale bar* = 20 μm. *C*, high-speed *in vitro* cosedimentation assay following AnxA2 or Src-CD protein incubation with (+) or without (-) preassembled K6-K17 filaments. Supernatant (*S*) and pellet (*P*) were separated, and immunoblotting was performed with antibodies against the indicated proteins. *D*, AnxA2 band intensities from *C* were quantified using the AlphaView SA software.

complex, treatment with EGF negatively impacts this interaction (Fig. 4, *B* and *C*).

We then examined the localization of AnxA2 and K17 to assess whether they are impacted by EGFR activation. This was of particular interest, as EGF treatment induces AnxA2 phosphorylation on residue Tyr-23 (Fig. 4*A*), correlating with the transfer of AnxA2 to the cell surface and endosomal compartments (27, 28). Prior to stimulation, endogenous AnxA2 showed a mostly diffused cytoplasmic staining pattern with membrane localization in growth factor-deprived A431 cells. In EGF-stimulated A431 cells, the signal for AnxA2 was lost from the K17 filament-rich perinuclear region and became enriched in the peripheral cytoplasm and outer cell membrane, indicating a potential loss of its interaction with K17 (Fig. 4*D* and supplemental Fig. S5). Together, the findings reported in Fig. 4 indicate that EGFR activation impacts the subcellular distribution of AnxA2, correlating with its phosphorylation on Tyr-23, and negatively regulates the AnxA2-K17 interaction.

AnxA2 Regulates Keratin Filaments—EGFR activation causes changes in keratin filament morphology (Fig. 2), whereas AnxA2 binds to K17-containing filaments (Fig. 3) but becomes disengaged following EGFR activation (Fig. 4). We

hypothesized that AnxA2 may play a protective role against the change in keratin solubility that parallels K17 filament remodeling. To test this hypothesis, AnxA2 was overexpressed in A431 cells, and endogenous K17 levels were examined (Fig. 5*A*). Relative to a vector control, A431 cells overexpressing AnxA2 showed higher levels of K17 in both the Triton-soluble and Triton-insoluble pools, suggesting that AnxA2 promotes K17 stability. Relative to the Triton-soluble pool, AnxA2 overexpression resulted in an enhanced enrichment of the Triton-insoluble K17. Indeed, compared with the vector control, AnxA2-overexpressing cells showed a decreased ratio of Triton-soluble to Triton-insoluble K17, indicating that AnxA2 overexpression results in filament stability (Fig. 5*B*). We next assessed the impact of AnxA2 overexpression on K17 upon EGF stimulation (Fig. 5, *C* and *D*). Similar to Fig. 5*A*, the basal levels (0 min) of K17 in the context of AnxA2 overexpression increased compared with the vector control. Interestingly, however, EGF-induced K17 increase in the Triton-soluble pool remained modest in AnxA2-overexpressing cells compared with the vector control (Fig. 5*C*). This implies that when overexpressed, AnxA2 suppresses EGFR-mediated change in K17 detergent solubility, consistent with our hypothesis that AnxA2
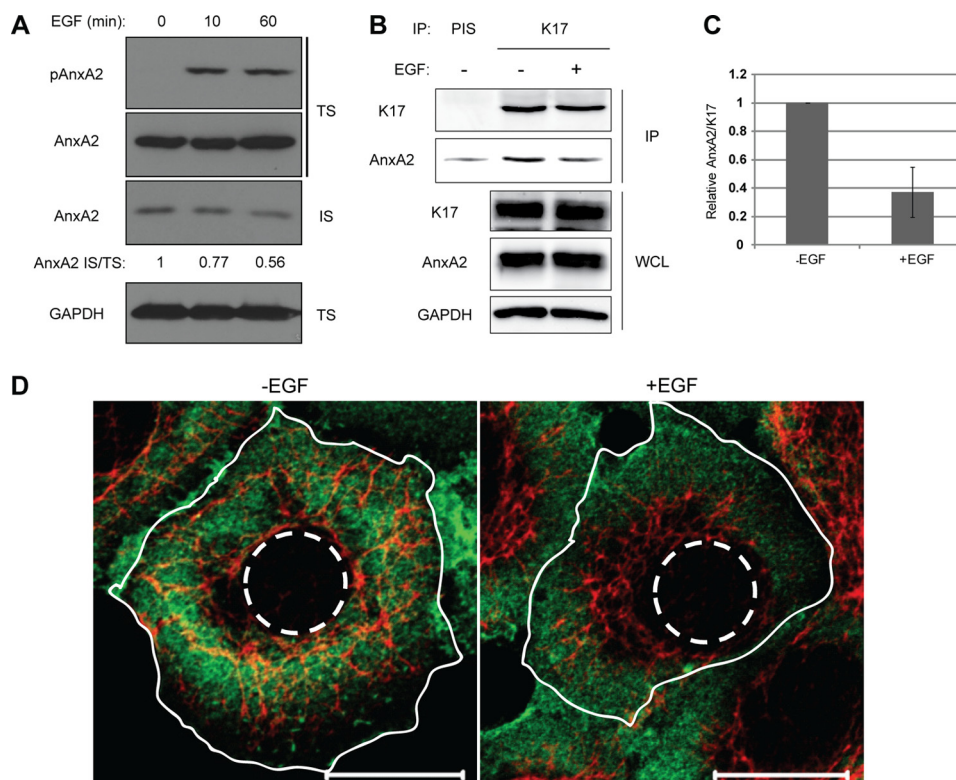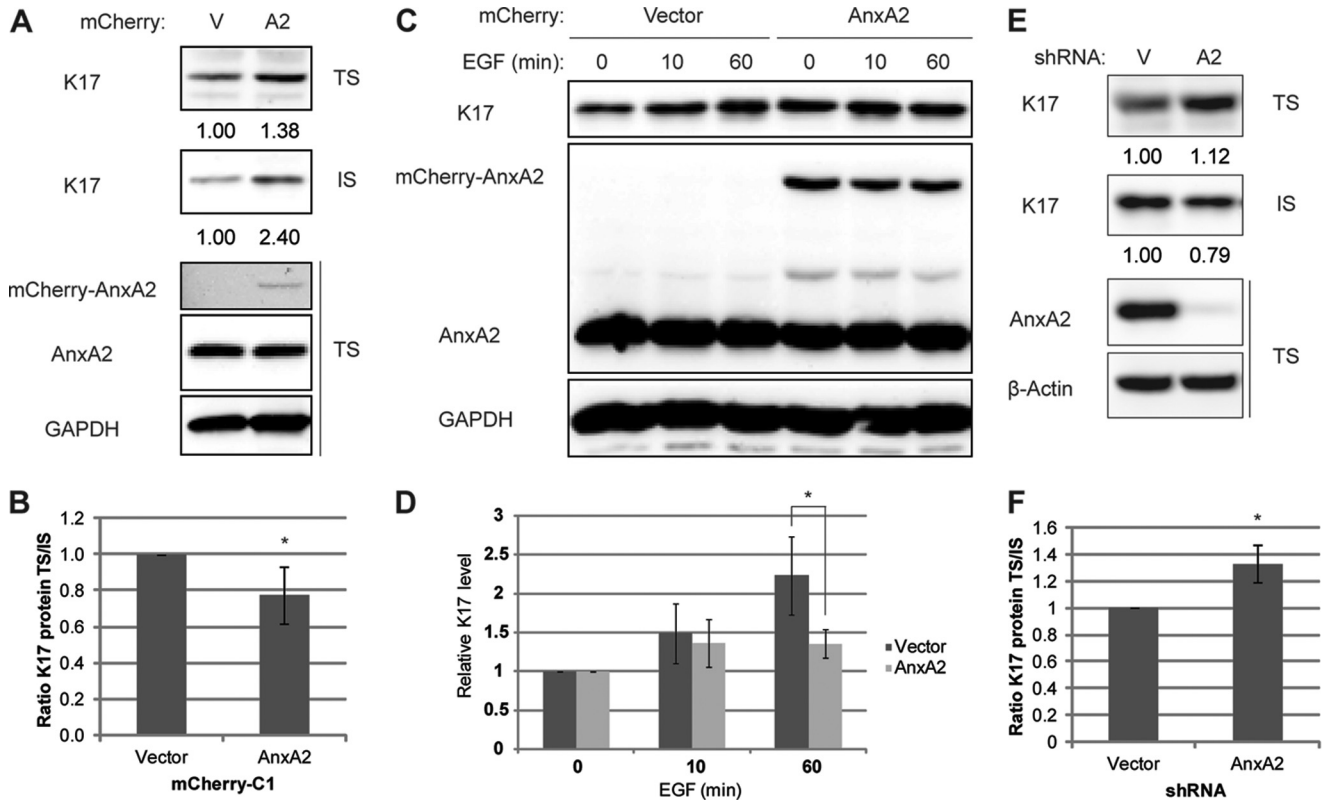
FIGURE 4. **EGF induces dissociation of K17 and AnxA2.** *A*, growth factor-deprived A431 cells were treated with 100 ng/ml EGF for the indicated time periods. Whole cell lysates were processed for Triton solubility, and immunoblotting was performed with antibodies against the indicated proteins. AnxA2 signal intensities were quantified using ImageJ. *B*, growth factor-deprived A431 cells were treated with (+) or without (-) 100 ng/ml EGF for 30 min. Immunoprecipitation was performed with anti-K17 antibody (*K17*) or preimmune serum (*PIS*) as a control, and immunoblotting was performed with antibodies against the indicated proteins. *C*, AnxA2 and K17 signal intensities from coimmunoprecipitation were quantified using ImageJ, and relative AnxA2/K17 is shown. *D*, growth factor-deprived A431 cells were treated with (+*EGF*) or without (-*EGF*) 100 ng/ml EGF for 30 min and then immunostained with anti-K17 (*red*) and anti-AnxA2 (*green*) antibodies. The plasma (*solid lines*) and nuclear (*dotted lines*) membranes are shown. *Scale bar* = 20 μm.

protects K17 filaments against reorganization. To expand on these overexpression studies, we then depleted AnxA2 in A431 cells using shRNA. Compared with the vector control, AnxA2-depleted cells showed a distinct partitioning of K17, with increased representation in the Triton-soluble pool and a decreased amount in the Triton-insoluble pool, suggesting decreased stability of K17-containing filaments (Fig. 5*E*). Therefore, the ratio of Triton-soluble to Triton-insoluble forms of K17 is higher in cells with reduced AnxA2 expression (Fig. 5*F*), an outcome that is opposite to what has been seen in AnxA2-overexpressing cells (*B*). Besides, AnxA2 depletion did not significantly affect EGF-induced K17 increase in the Triton-soluble pool (supplemental Fig. S6). This is likely due to the already elevated level of Triton-soluble K17 and/or low level of Triton-insoluble K17 available to be remodeled in the context of EGF treatment. Overall, these data suggest that AnxA2 regulates K17 stability and prevents K17 filament remodeling.

K17 Regulates AnxA2—Next, we transiently and partially silenced K17 expression in A431 cells to investigate whether it impacts AnxA2 regulation. Two different shRNA against K17 (K17C and K17D) were designed and tested in A431 cells, along with vector (V) and non-sense (NS) controls. The K17C and K17D shRNA successfully knocked down endogenous K17 levels to ~40 and 60%, respectively, compared with controls (Fig. 6*A*). Such K17 silencing had very little, if any, effect on AnxA2 levels in the Triton-soluble pool. In contrast, the levels of AnxA2 in the Triton-insoluble fraction were reduced. To fur-

ther test the possibility that K17 may also promote AnxA2 stability, we next assessed the detergent solubility of AnxA2 upon K17 and K5 overexpression in BHK-21 fibroblasts, which lack endogenous keratin expression. Increasing amounts of K17 resulted in increasing levels of AnxA2 in the detergent-insoluble pool in dual K5/K17-transfected BHK-21 cells (Fig. 6*B*). These results indicate that K17 is able to impact the expression level and subcellular partitioning of AnxA2.

K17 Facilitates Phosphorylation of AnxA2—AnxA2 and K17 show increased expression during *in vitro* cellular carcinogenesis from oral epithelial cells to squamous cell carcinoma (29). Besides, the Src-dependent phosphorylation of the tyrosine of AnxA2 plays a role in tumor progression and metastasis in a pancreatic cancer model (30). Therefore, we decided to examine Tyr-23 phosphorylation on AnxA2 in A431 cells, and a clone in which the K17C shRNA is stably expressed. When such cells were stimulated with EGF to induce AnxA2 phosphorylation, K17 silencing was associated with decreased AnxA2 phosphorylation in response to EGF (Fig. 7*A*). To confirm the impact of the expression status of K17 on AnxA2 phosphorylation, we utilized primary keratinocytes isolated from mice that are hemi- or homozygous for a *K17* null allele. Similar to our findings with A431 stable transfectants, *K17* null primary keratinocytes consistently showed reduced AnxA2 phosphorylation (Fig. 7, *B* and *C*). Interestingly, reduced AnxA2 phosphorylation in K17-depleted or null cells occurred without any change in EGFR phosphorylation (supplemental Fig. S7). Taken

FIGURE 5. **AnxA2 stabilizes keratin filaments and delays EGF-induced change in keratin solubility.** *A–D*, mCherry-AnxA2 (*AnxA2*) or vector control (*V*) was transiently transfected into A431 cells. *A*, whole cell lysates were processed for Triton solubility. *B*, quantitation of *A*. Relative K17 levels in TS/IS for cells expressing vector control or mCherry-AnxA2 are shown. *, $p < 0.05$. *C*, growth factor-deprived cells were treated with 100 ng/ml EGF for the indicated time periods, and whole cell lysates were prepared in Triton lysis buffer. Immunoblotting was performed with antibodies against the indicated proteins, and signal intensities were quantified using AlphaView SA. *D*, quantitation of *C*. Relative K17 levels were normalized to those from 0 min EGF stimulation. *, $p < 0.05$. *E*, whole cell lysates of A431 cells stably expressing vector control or AnxA2 shRNA were processed for Triton solubility. *F*, quantitation of *E*. Relative K17 levels in TS/IS are shown. *, $p < 0.05$.
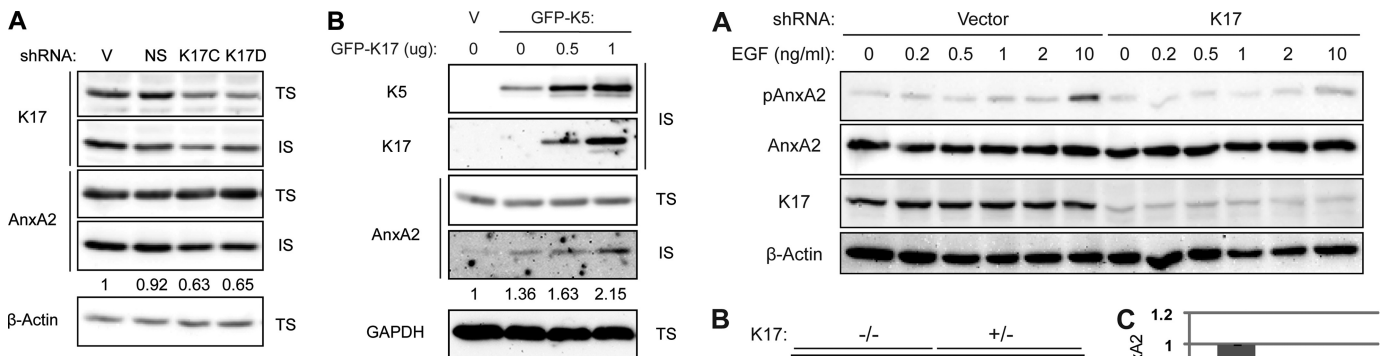
FIGURE 6. **K17 modulates AnxA2 levels in the Triton-insoluble pool.** *A*, shRNAs targeting K17 (*K17C* and *K17D*), vector (*V*), or non-sense control (*NS*) were transiently transfected into A431 cells. *B*, GFP-K5, K17, or a vector control were transiently transfected into BHK-21 cells. Whole cell lysates were processed for Triton solubility, and immunoblotting was performed with antibodies against the indicated proteins. AnxA2 (*IS*) signal intensities were quantified using the AlphaView SA software.

FIGURE 7. **K17 impacts the extent of AnxA2 Y23 phosphorylation.** *A*, A431 cells with stable knockdown of K17 or vector control were growth factor-deprived and stimulated with the indicated concentration of EGF for 30 min. *B*, skin keratinocytes were obtained from K17$^{+/-}$ or K17$^{-/-}$ newborn mice ($n = 4$ each) and seeded for primary culture. Whole cell lysates were prepared in Triton lysis buffer. Immunoblotting was performed with antibodies against the indicated proteins. *C*, pAnxA2 and AnxA2 signal intensities from *B* were quantified using the AlphaView SA software.

together, these findings showed that K17 impacts AnxA2 phosphorylation.

DISCUSSION

The keratin family of intermediate filament proteins is involved in multiple cellular functions, including tumorigenesis (8), in addition to providing vital structural support when polymerized and organized into a cross-linked network (2, 22, 31). Identifying new binding partners and regulatory mecha-

nisms can assist toward elucidating new keratin roles that might impact cancer progression and the pathophysiology of other relevant diseases. Although much effort has been made to

understand oncogenic signaling networks in cancer, disappointingly little is known about why "key marker proteins" such as K17 are induced or up-regulated in such settings and whether there exists a correlation between K17 expression and signaling pathways such as EGFR and its downstream effectors.

Keratin solubility in detergents is closely correlated to the intracellular distribution, and organization, of keratin filaments (32). Our study demonstrates that EGFR activity regulates K17 by modulating its detergent solubility. This event is specific, as partner K5 is unaffected by EGFR status. Although the up-regulation of Triton-soluble K17 following EGF stimulation is partly a transcriptional event (data not shown and Ref. 11), EGF also causes rapid changes in keratin filament organization in mouse embryonic epithelial cells (33), rat hepatocytes (34), and human colon cancer cells (35). K6, another type II assembly partner for K17, is expressed in very low amounts in A431 cells (data not shown and Ref. 36) and therefore cannot be the principal partner of K17 in this setting. The specific change in K17 protein levels and solubility may therefore reflect a specialized function for K17 downstream from EGFR activation.

In an effort to define the mechanism underlying EGFR-mediated change in K17 filament attributes, we identified AnxA2 to be a K17-binding partner in cultured cells and in the setting of purified proteins *in vitro*. AnxA2 is implicated in many biological processes, including those involved in cancer progression. *In situ*, AnxA2 expression is high in the highly proliferating basal layer of normal epidermis but low in the suprabasal layers (37, 38). AnxA2 is often dysregulated in cancers and has been used as a prognostic marker (reviewed in Ref. 39). RNAi-mediated silencing of AnxA2 impairs the migration of human epithelial colorectal adenocarcinoma cells (40) and glioma cells (41) and reduces the invasiveness of breast cancer cells (18), all highlighting the potential importance of AnxA2 in cancer progression.

The AnxA2-K17 interaction is attenuated after EGFR activation, correlating with dissociation of AnxA2 from the K17-rich filament pool. Altering AnxA2 expression affects K17 levels within the filament-rich Triton-insoluble pool, and AnxA2 overexpression suppresses the EGFR-mediated change in K17 detergent solubility. Similarly, modulation of K17 steady-state levels causes change in the extent of AnxA2 association with the K17-rich filament pool and with AnxA2 phosphorylation. AnxA2 is a substrate of both Src and PKC (42), and is required for Src-dependent trafficking and Src-mediated transformation (43). Further, Src-mediated AnxA2 Y23 phosphorylation plays a role in cell scattering and branching morphogenesis by promoting actin cytoskeletal dynamics (44). Phosphorylation of AnxA2 at Tyr-23 has also been shown to be required for the progression and metastasis of pancreatic ductal adenocarcinoma (30). Although the extent of AnxA2 Y23 phosphorylation is affected in K17 knockdown cells, we find that Src activity remains unchanged (data not shown). Therefore, it is likely that the regulatory role of K17 on AnxA2 lies downstream of Src activation. Our findings suggest that K17 impacts AnxA2 phosphorylation via its effect on its distribution and/or partitioning to the soluble pool. Because AnxA2 binds to K17 filaments and modulating K17 expression alters AnxA2 levels in the keratin-rich Triton-insoluble pool, it appears likely that K17 regulates

AnxA2 and serves as a scaffold, facilitating AnxA2 phosphorylation. In addition to cytoskeletal proteins, the Triton-insoluble protein pool contains other "protein subproteomes," such as lipid rafts, where AnxA2 has been shown to occur (15). Therefore, it is possible that K17·AnxA2 complexes occur as part of the cytoskeletal network as well as in plasma membrane-associated lipid rafts. It is worth noting that although most of the cellular AnxA2 content is Triton-soluble, most of the content of K17 is Triton-insoluble. Therefore, changes in the levels of K17 protein in the Triton-soluble pool (Figs. 2*B* and 5) and in AnxA2 protein in the Triton-insoluble pool (Figs. 4*A* and 6) must only involve a small fraction of their overall amount present in the cell. The fact that K17 impacts Tyr-23 phosphorylation on AnxA2 suggests that however modest it is in quantitative terms, the K17-AnxA2 interaction likely impacts a highly specialized fraction of each protein in a spatial and temporal fashion. As AnxA2 stabilizes K17 filament (Fig. 5), and AnxA2 colocalization along K17 is not continuous along the K17 filament but punctate (Fig. 3*B*), further study of the underlying mechanism(s) and the biological relevance of this dynamic interaction now represent issues worth pursuing. Meanwhile, the findings reported here contribute to the understanding of the molecular mechanism downstream of an oncogenic signaling pathway and identified AnxA2 as a novel regulator of keratin filaments.

REFERENCES

1. Gu, L. H., and Coulombe, P. A. (2007) Keratin function in skin epithelia: a broadening palette with surprising shades. *Curr. Opin. Cell Biol.* **19,** 13–23
2. Kim, S., and Coulombe, P. A. (2007) Intermediate filament scaffolds fulfill mechanical, organizational, and signaling functions in the cytoplasm. *Genes Dev.* **21,** 1581–1597
3. Coulombe, P. A., Hutton, M. E., Letai, A., Hebert, A., Paller, A. S., and Fuchs, E. (1991) Point mutations in human keratin 14 genes of epidermolysis bullosa simplex patients. Genetic and functional analyses. *Cell* **66,** 1301–1311
4. Coulombe, P. A., Kerns, M. L., and Fuchs, E. (2009) Epidermolysis bullosa simplex. A paradigm for disorders of tissue fragility. *J. Clin. Invest.* **119,** 1784–1793
5. Kim, S., Kellner, J., Lee, C. H., and Coulombe, P. A. (2007) Interaction between the keratin cytoskeleton and eEF1Bγ affects protein synthesis in epithelial cells. *Nat. Struct. Mol. Biol.* **14,** 982–983
6. Kim, S., Wong, P., and Coulombe, P. A. (2006) A keratin cytoskeletal protein regulates protein synthesis and epithelial cell growth. *Nature* **441,** 362–365
7. Nielsen, T. O., Hsu, F. D., Jensen, K., Cheang M., Karaca, G., Hu, Z., Hernandez-Boussard, T., Livasy, C., Cowan, D., Dressler, L., Akslen, L. A., Ragaz, J., Gown, A. M., Gilks, C. B., van de Rijn, M., and Perou, C. M. (2004) Immunohistochemical and clinical characterization of the basal-like subtype of invasive breast carcinoma. *Clin. Cancer Res.* **10,** 5367–5374
8. Depianto, D., Kerns, M. L., Dlugosz, A. A., and Coulombe, P. A. (2010) Keratin 17 promotes epithelial proliferation and tumor growth by polarizing the immune response in skin. *Nat. Genet.* **42,** 910–914
9. Jiang, C. K., Magnaldo, T., Ohtsuki, M., Freedberg, I. M., Bernerd, F., and Blumenberg, M. (1993) Epidermal growth factor and transforming growth factor α specifically induce the activation- and hyperproliferation-associated keratins 6 and 16. *Proc. Natl. Acad. Sci. U.S.A.* **90,** 6786–6790
10. Wang, Y. N., and Chang, W. C. (2003) Induction of disease-associated keratin 16 gene expression by epidermal growth factor is regulated

through cooperation of transcription factors Sp1 and c-Jun. *J. Biol. Chem.* **278,** 45848–45857

11. Amit, I., Citri, A., Shay, T., Lu, Y., Katz, M., Zhang, F., Tarcic, G., Siwak, D., Lahad, J., Jacob-Hirsch, J., Amariglio, N., Vaisman, N., Segal, E., Rechavi, G., Alon, U., Mills, G. B., Domany, E., and Yarden, Y. (2007) A module of negative feedback regulators defines growth factor signaling. *Nat. Genet.* **39,** 503–512

12. Paladini, R. D., and Coulombe, P. A. (1998) Directed expression of keratin 16 to the progenitor basal cells of transgenic mouse skin delays skin maturation. *J. Cell Biol.* **142,** 1035–1051

13. Blagoev, B., Kratchmarova, I., Ong, S. E., Nielsen, M., Foster, L. J., and Mann, M. (2003) A proteomics strategy to elucidate functional protein-protein interactions applied to EGF signaling. *Nat. Biotechnol.* **21,** 315–318

14. Thelemann, A., Petti, F., Griffin, G., Iwata, K., Hunt, T., Settinari, T., Fenyo, D., Gibson, N., and Haley, J. D. (2005) Phosphotyrosine signaling networks in epidermal growth factor receptor overexpressing squamous carcinoma cells. *Mol. Cell. Proteomics* **4,** 356–376

15. Oliferenko, S., Paiha, K., Harder, T., Gerke, V., Schwärzler, C., Schwarz, H., Beug, H., Günthert, U., and Huber, L. A. (1999) Analysis of CD44-containing lipid rafts. Recruitment of annexin II and stabilization by the actin cytoskeleton. *J. Cell Biol.* **146,** 843–854

16. Gu, L. H., and Coulombe, P. A. (2005) Defining the properties of the nonhelical tail domain in type II keratin 5. Insight from a bullous disease-causing mutation. *Mol. Biol. Cell* **16,** 1427–1438

17. Pan, X., Kane, L. A., Van Eyk, J. E., and Coulombe, P. A. (2011) *J. Biol. Chem.* **286,** 42403–42413

18. Zhang, F., Zhang, L., Zhang, B., Wei, X., Yang, Y., Qi, R. Z., Ying, G., Zhang, N., and Niu, R. (2009) Anxa2 plays a critical role in enhanced invasiveness of the multidrug-resistant human breast cancer cells. *J. Proteome Res.* **8,** 5041–5047

19. Choi, Y. B., and Nicholas, J. (2008) Autocrine and paracrine promotion of cell survival and virus replication by human herpesvirus 8 chemokines. *J. Virol.* **82,** 6501–6513

20. Bernot, K. M., Coulombe, P. A., and Wong, P. (2004) Skin. An ideal model system to study keratin genes and proteins. *Methods Cell Biol.* **78,** 453–487

21. McGowan, K. M., and Coulombe, P. A. (1998) Onset of keratin 17 expression coincides with the definition of major epithelial lineages during skin development. *J. Cell Biol.* **143,** 469–486

22. Lee, C. H., and Coulombe, P. A. (2009) Self-organization of keratin intermediate filaments into cross-linked networks. *J. Cell Biol.* **186,** 409–421

23. Ma, L., Yamada, S., Wirtz, D., and Coulombe, P. A. (2001) A "hot-spot" mutation alters the mechanical properties of keratin filament networks. *Nat. Cell Biol.* **3,** 503–506

24. Hayes, M. J., Shao, D., Bailly, M., and Moss, S. E. (2006) Regulation of actin dynamics by annexin 2. *EMBO J.* **25,** 1816–1826

25. Ma, A. S., Bystol, M. E., and Tranvan, A. (1994) *In Vitro* modulation of filament bundling in F-actin and keratins by annexin II and calcium. *In vitro Cell. Dev. Biol. Anim.* **30A,** 329–335

26. Garbuglia, M., Bianchi, R., Verzini, M., Giambanco, I., and Donato, R. (1995) Annexin II2-p11(2) (calpactin I) stimulates the assembly of GFAP in a calcium- and pH-dependent manner. *Biochem. Biophys. Res. Commun.* **208,** 901–909

27. Morel, E., and Gruenberg, J. (2009) Annexin A2 binding to endosomes and functions in endosomal transport are regulated by tyrosine 23 phosphorylation. *J. Biol. Chem.* **284,** 1604–1611

28. Deora, A. B., Kreitzer, G., Jacovina, A. T., and Hajjar, K. A. (2004) An annexin 2 phosphorylation switch mediates p11-dependent translocation of annexin 2 to the cell surface. *J. Biol. Chem.* **279,** 43411–43418

29. Zhong, L., Zhang, L., Yang, X., Pan, H., Zhou, X., Wei, K., Ye, D., Jiang, Q., Chen, W., and Zhang, Z. (2009) Comparative proteomic analysis of differentially expressed proteins in an *in vitro* cellular carcinogenesis model of oral squamous cell carcinoma. *Proteomics Clin. Appl.* **3,** 322–337

30. Zheng, L., Foley, K., Huang, L., Leubner, A., Mo, G., Olino, K., Edil, B. H., Mizuma, M., Sharma, R., Le, D. T., Anders, R. A., Illei, P. B., Van Eyk, J. E., Maitra, A., Laheru, D., Jaffee, E. M. (2011) Tyrosine 23 phosphorylation-dependent cell surface localization of annexin A2 is required for invasion and metastases of pancreatic cancer. *PLoS ONE* **6,** e19390

31. Toivola, D. M., Strnad, P., Habtezion, A., and Omary, M. B. (2010) Intermediate filaments take the heat as stress proteins. *Trends Cell Biol.* **20,** 79–91

32. Kasahara, K., Kartasova, T., Ren, X. Q., Ikuta, T., Chida, K., and Kuroki, T. (1993) Hyperphosphorylation of keratins by treatment with okadaic acid of BALB/MK-2 mouse keratinocytes. *J. Biol. Chem.* **268,** 23531–23537

33. Keski-Oja, J., Lehto, V. P., and Virtanen, I. (1981) Keratin filaments of mouse epithelial cells are rapidly affected by epidermal growth factor. *J. Cell Biol.* **90,** 537–541

34. Baribault, H., Blouin, R., Bourgon, L., and Marceau, N. (1989) Epidermal growth factor-induced selective phosphorylation of cultured rat hepatocyte 55-kD cytokeratin before filament reorganization and DNA synthesis. *J. Cell Biol.* **109,** 1665–1676

35. Ku, N. O., and Omary, M. B. (1997) Phosphorylation of human keratin 8 in vivo at conserved head domain serine 23 and at epidermal growth factor-stimulated tail domain serine 431. *J. Biol. Chem.* **272,** 7556–7564

36. Moll, R., Franke, W. W., Schiller, D. L., Geiger, B., and Krepler, R. (1982) The catalog of human cytokeratins. Patterns of expression in normal epithelia, tumors and cultured cells. *Cell* **31,** 11–24

37. Munz, B., Gerke, V., Gillitzer, R., and Werner, S. (1997) Differential expression of the calpactin I subunits annexin II and p11 in cultured keratinocytes and during wound repair. *J. Invest. Dermatol.* **108,** 307–312

38. Kim, T. T., Chen, C. T., and Huang, C. C. (1998) Expression of annexin II in human middle ear cholesteatoma. *Otolaryngol. Head Neck Surg.* **118,** 324–328

39. Sharma, M. C., and Sharma, M. (2007) The role of annexin II in angiogenesis and tumor progression. A potential therapeutic target. *Curr. Pharm. Des.* **13,** 3568–3575

40. Babbin, B. A., Parkos, C. A., Mandell, K. J., Winfree, L. M., Laur, O., Ivanov, A. I., and Nusrat, A. (2007) Annexin 2 regulates intestinal epithelial cell spreading and wound closure through Rho-related signaling. *Am. J. Pathol.* **170,** 951–966

41. Tatenhorst, L., Rescher, U., Gerke, V., and Paulus, W. (2006) Knockdown of annexin 2 decreases migration of human glioma cells *in vitro*. *Neuropathol. Appl. Neurobiol.* **32,** 271–277

42. Rothhut, B. (1997) Participation of annexins in protein phosphorylation. *Cell Mol. Life Sci.* **53,** 522–526

43. Hayes, M. J., and Moss, S. E. (2009) Annexin 2 has a dual role as regulator and effector of v-Src in cell transformation. *J. Biol. Chem.* **284,** 10202–10210

44. de Graauw, M., Tijdens, I., Smeets, M. B., Hensbergen, P. J., Deelder, A. M., and van de Water, B. (2008) Annexin A2 phosphorylation mediates cell scattering and branching morphogenesis via cofilin activation. *Mol. Cell Biol.* **28,** 1029–1040